International Journal of Science and Research (IJSR)
ISSN (Online): 2319-7064
Index Copernicus Value (2013): 6.14 | Impact Factor (2013): 4.438

Size Effect of R.C Beams Flexurally Strengthened with Different Types of FRP Sheets against Flexural Loads

Mohammed M. M. Rashwan[1], Hesham M. A. Diab[2], Tarek A. A. KHALED[3].

[1]Professor of Structural Engineering, Civil Eng. Dept., Assuit Univ., 71516 Assuit

[2]Associate Professor of Structural Engineering, Civil Eng. Dept., Assuit University, 71516 Assuit

[3]Demonstrator, Civil Eng. Dept., Assuit University, 71516 Assuit

Abstract: ***In this study, a series of reinforced concrete beams were carried out to determine the size effect of the beams strengthened with different types of fiber reinforced polymer sheets (FRP). Two types of FRP sheets were considered in this study; Carbon and Glass fiber reinforced polymer sheets (CFRP and GFRP). FRP sheets were bonded to the soffit of the beams using a two-part Epoxy. These two types of FRP sheets were used to allow a variety of fabric stiffnesses and strengths to be studied. Also, this study introduced a new type of anchor to improve the efficiency of the FRP-strengthened beams and to prevent the anchor delamination of the FRP sheets. The results show that the strengthening system increases the ultimate capacity of the FRP-strengthened beams. Also, this increase depends on many parameters such as the type of the FRP sheets and size of the tested beams. Moreover, the beam size has significantly effected on the ductility of testing beams which increases as the size of beams decreases.***

Keywords: Carbon fiber reinforced polymer sheets, glass fiber reinforced polymer sheets, debonding, anchorage system.

1. Introduction

Strengthening of concrete structures using fiber reinforced polymer (FRP) composites has been widely accepted as a promising alternative to conventional strengthening methods; along with high structural effectiveness, composite materials are light and easy to install, their application does not imply loss of space and, in some cases, it can be performed without interrupting the use of the structure. The effectiveness of such strengthening technique is dependent on many parameters such as, types and properties of FRP, bonding method of FRP, and loading type of the structure [1, 2 and 3].

Therefore, Extensive researches have been directed to investigate the performance of FRP-strengthened concrete structures. Most of these previous studies showed significant increases in the load capacity of the strengthened structures. However, this strengthening type hasn't problem free. Recent studies showed that the performance of FRP-strengthened beams dependent mainly on the FRP type. The brittle behavior of FRP-strengthened beam can be improved by using low modulus of elasticity FRP and by using a flexible type of epoxy [4]. Moreover, Abdelhady Hosny et al. [5] and Aprile et al. [6] improved ductility of FRP-strengthened beams by using a combination of FRP such as GFRP and CFRP or using low stiffness FRP [7].

The effect of CFRP thickness and length on the failure load and ductility is studied, and the values of initial cracking load, ultimate load, stiffness, ductility and fibre stresses are presented [8, 9 and 2]. These studies indicated that significant increase in the flexural strength can be achieved by bonding GFRP plates to the tension face of reinforced concrete beams. Also, the gain in the ultimate capacity of the FRP-strengthened beams was more significant in beams with lower steel reinforcement ratios. In addition, plating reduces the crack size in the beams at all load levels. Moreover, the crack pattern has significantly affected by the type of the FRP [10]

Most of FRP-strengthening structures have shown significant increases in the ultimate strength. However, the low efficiency of the FRP sheets has been observed due to the possibility of premature debonding failure [8, 10, 11, 12 and 13]. It is understood that the bond strength of FRP materials can be improved when sufficient anchorage is provided and such provisions have been acknowledged to delay or prevent the critical mode of FRP debonding failure [14 and 15]. Anchors made from rolled fiber sheets or bundled loose fibers are a promising form of anchorage because they can be applied to wide FRP-strengthened structural elements such as slabs and walls. They are discrete and do not suffer from the same constraints as U-jackets. Such anchors are referred to as FRP spike anchors, fiber anchors, fiber bolts, and FRP dowels, among other names, but are herein collectively referred to as FRP anchors [16].

There is controversy concerning the size effect of FRP-strengthened beams and there are limited experimental studies which solve this problem. Maalej et al, [17] carried out an experimental program to study the effect of beam size on the performance of FRP-strengthened beams and they concluded that the size of the beams and the amount of the FRP result in an increase of the interfacial shear stress in the FRP curtailment region. However, the peak shear stresses are not high enough to cause a change in the failure mode of the beams and the size of the beam does not affect the flexural capacity of beams. However, their study considered a constant steel ratio and constant fiber to steel ratio for different beams.

Till now, there are limited laboratory tests considering the size effect supporting the validity of the results obtained by Maalej et al, [17]. Therefore, our experimental program has been carried out to increase the experimental results considering the size effect and to consider different parameters such as the steel ratio, the FRP-steel ratio, and the type of the FRP.

2. Experiments

2.1. Test Specimens

The experimental program included a total of three small-scale beams, two medium-scale beams and two large-scale beams. The details of the experimental program are given in Table 1. The details of reinforcement are shown in Fig. 1.

Table 1: Beam list and strengthening details

Beam	Length "m"	Area of section "mm2"	External strengthened	Anchorage	Type of FRP sheet	scale
A1	1.80	120*200	Not strengthened	None	————	Small scale
A2	1.80	120*200	Strengthened	End anchorage	CFRP	Small scale
A3	1.80	120*200	Strengthened	End anchorage	GFRP	Small scale
B1	2.80	150*300	Not strengthened	None	————	Med. scale
B2	2.80	150*300	Strengthened	End anchorage	CFRP	Med. scale
C1	4.30	200*400	Not strengthened	None	————	Large scale
C2	4.30	200*400	Strengthened	End anchorage	CFRP	Large scale

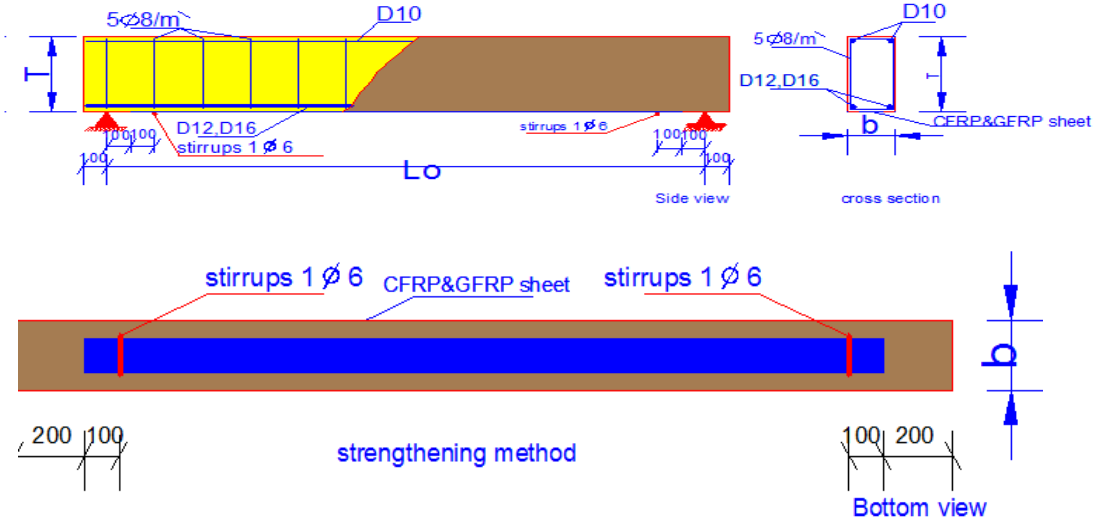

Figure 1: Details of specimens (dimensions in mm)

2.2. Material Properties

The 28-day compressive strength is 25 MPa which obtained using (150*150*150) mm3 cubes. The proportions of concrete mix are shown in Table 2. High tensile steel (360/520) is used for the longitudinal reinforcement, and normal mild steel (240/350) is used for transversal reinforcement (stirrups). Sika Wrap Hex 230C is a unidirectional carbon fiber fabric were used for the strengthening of the RC beams. Sika dur 330 epoxy was used to bond the carbon fiber reinforced polymer (CFRP) and glass fiber reinforced polymer (GFRP) which are used to strengthen the RC beams. The mechanical properties of the CFRP composite strips, and the epoxy resin is based on the manufacturer's data sheets and appear in Table 3. It's observed from a tension test that tensile strength for CFRP was 3045 MPa. Tension test-setup and tested specimen are shown in Fig.2.

Table 2: Characteristics of concrete mix design

Concrete compressive strength (MPa)	Mix proportions kgf/m3			
	W	C	S	G
25	212	400	651	1142

Figure 2.a. Machine test.

Figure 2 b. Test specimens.
Figure 2: Tension test on FRP coupons.

Table 3: Mechanical properties of FRP materials

Material	Modulus of elasticity GPa	Tensile strength MPa	Fiber orientation	Thickness mm	Elongation at failure	Surface mass g/m2
GFRP/fiber SikaWrap430G	76	2470	Unidirectional	0.17	2.8%	430
CFRP/fiber SikaWrap230C	230	3045	Unidirectional	0.13	1.5%	230
Sika330 epoxy	3.8	30	————	1.0	0.9%	500

2.3. Test setup

The test setup, the various monitoring devices, and their location along the beam appear in Fig. 3. The beams were tested using a displacement control with two types of machines 600 kN and 5000 kN capacity. The monitoring devices include linear voltage displacement transducers (LVDT) and strain gauges are shown in Fig. 3. These devices are divided into four groups as follows:

1. Measurement of the vertical deflections. LVDT, denoted by LVDT was located at midspan.
2. Measurement of the strains of the internal steel rebars. This is achieved using two strain gauges (denoted by SSG1 and SSG 2) bonded to the internal steel bars.
3. Measurement of the strains of the FRP strip. This is accomplished using a double strain gauge (FSG1 and FSG2) bonded to the outer face of the FRP strip at the middle and a quarter of the beam.
4. The last strain, denoted by CSG and, was bonded at the compression zone for concrete in the middle of the beam (Fig. 3).

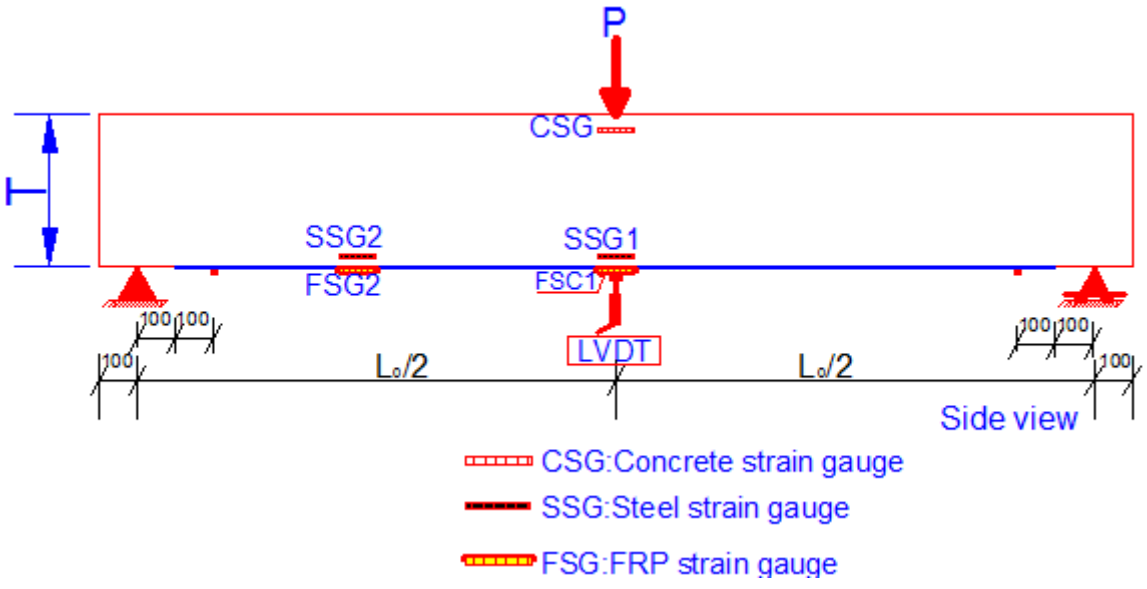

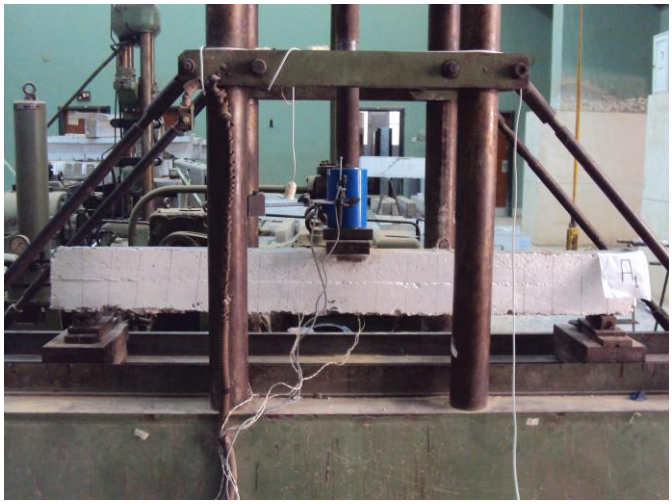

Figure 3: Test set-up.

2.4. Strengthening Procedure

All beams were strengthened using externally bonded CFRP and GFRP sheets. The strengthening procedures included surface preparation, application of a priming adhesive layer, and bonding of the FRP strip. The surface preparation included intensive cleaning, removal of unstable particles, and mechanical roughening down to aggregate surface. Following this stage, a 1–2 mm thick priming layer of the same adhesive used for bonding the CFRP and GFRP sheets has been applied on the roughened surface and cured in the open air for 24 h. Next, the FRP sheets were impregnated with Sika dur 330 epoxy and then, attached in position on the tensile face of each beam, and fastened with a roller. Finally, the adhesive and the epoxy resin were cured for at least 7 days before loading. Fig.4. shows the preparation of the experimental beams. All Strengthened beams have the same CFRP&GFRP reinforcement ratio (10% from tensile steel with a constant breath equals 2/3 width of the cross section. The stirrups of anchor used to fix the CFRP&GFRP sheets prevent slippage using a surface curvature, which increases the friction force. As shown in Fig 4.c.

a. Surface preparation.

b. Bonding of the FRP sheet.

c. Anchorage system

Figure 4:The strengthening procedure

3. Experimental results

In Table (4) the values of cracking, ultimate and debonding loads and maximum CFRP&GFRP sheets strain for all test specimens are given, also it includes the failure mode of all tested beams. These failure modes are termed: Type (1) tension failure by yielding of the steel in tension for unstrengthened beams or by rupture of the FRP laminate after yielding of the steel in tension for strengthening beams, Type (2) flexural failure by crushing of compressive concrete which could happen before or after yielding of tensile steel reinforcement and Type (3) interfacial debonding induced by flexural shear crack.

Table 4: Summary of test results

Specimens	Cracking		Debonding		Ultimate		Max. CFRP and GFRP sheet stains (με)	Ratio of load increase (%).	Failure mode
	Pcr (kN)	Defl. (mm)	Pd (kN)	Defl. (mm)	Pu (kN)	Defl. (mm)			
A1	8.0	1.31	-	-	41.0	59.00	-	-	**Tension**
A2	12.0	2.12	52	16.69	55.5	29.90	10631	35.36	**Flexural**
A3	11.0	1.65	-	-	48.0	28.67	7640	17.07	**Flexural shear**
B1	10.0	1.94	-	-	45.5	40.19	-	-	**Tension**
B2	12.0	2.50	53.0	20.08	56.5	30.50	8086	25.27	**Tension**
C1	20.0	1.20	-		71.5	85.30	-	-	**Tension**
C2	22	1.1	83.0	24.70	87.5	37.50	3590	22.38	**Tension**

3.1. Crack patterns and failure modes

From the experimental tests, a typical pattern of crack formation was observed. The first flexural crack occurred in the mid-span of the beam, and was followed by the formation and propagation of many smaller cracks which were symmetrically distributed about the mid-span of the beam. The crack formation pattern was similar for all the tested beams. Both deflection and cracking were reduced in proportion to the type of FRP sheets and scale of beams. Furthermore, the presence of the bonded CFRP and GFRP sheets helped to distribute the flexural cracks more evenly along the length of the beams resulting in smaller crack width. This is similar to the trend reported previously by other researchers. These flexural cracks continued to propagate with shear cracks at higher load levels.

All control beams failed in the conventional mode of steel yielding. The failure mode for all CFRP-strengthened beams was beginning with an intermediate flexural crack induced interfacial debonding. Debonding propagates toward support. Upon debonding, a very thin layer of concrete and aggregate generally remained attached to the CFRP sheet. But the spread of cracks was larger with the appearance largely of shear cracks at small scale, and therefore need more strengthening the strongest to avoid the collapse of the shear in small-scale beams. Mode of failure of control beams are shown in Fig. 5.

Figure 5: Mode of failure of control beams (A1, B1and C1).

3.2. Flexural behavior and strengthening effects

3.2.1 Control beams: results and discussion

3.2.1.1 Beam A1

The results for beam A1 appear in Fig. 6.a. This includes a linear response up to the cracking load of 8.0 kN Almost identical cracks about the middle up the start of the shear crack at load 24 kN (60%) of the total load at 300 mm from the support, a cracked behavior up to the yielding point of the internal rebars at 38 kN, and a long inelastic response up to the ultimate load of 41 kN Loading of beam A1 was stopped at a deflection of about 59 mm (1/31 of the span) and the residual deflection after unloading was 57 mm.

3.2.1.2 Beam B1

The results for beam B1 appear in Fig. 6.a. and reveal a cracking load of 10 kN, and an ultimate load of 45.5 kN these values are higher than the ones observed in beam A1 due to the larger cross sectional area. The cracking pattern of beam B1 includes vertical flexural cracks around midspan. Failure of beam B1 occurred due to tension failure. There are no cracks in the shear span and further crack about midspan at a distance of 700 mm at load 32 kN. Loading of beam B1 was stopped at a deflection of about 40.19 mm (1/70 of the span).

3.2.1.3 Beam C1

The results for beam C1 appear in Fig. 6.a. and reveal a cracking load of 18 kN, and an ultimate load of 71.5 kN these values are higher than the ones observed in beam A1 and B1 due to the larger cross sectional area. The cracking pattern of beam C1 includes vertical flexural cracks around midspan. Failure of beam C1 occurred due to tension failure. There are no cracks in the shear span and further crack about midspan at a distance of 1200 mm at load 45 kN. Loading of beam C1 was stopped at a deflection of about 85.3 mm (1/50.4 of the span). Load versus compression strain for the control beams A1, B1, and C1 is shown in Fig. 6. b.

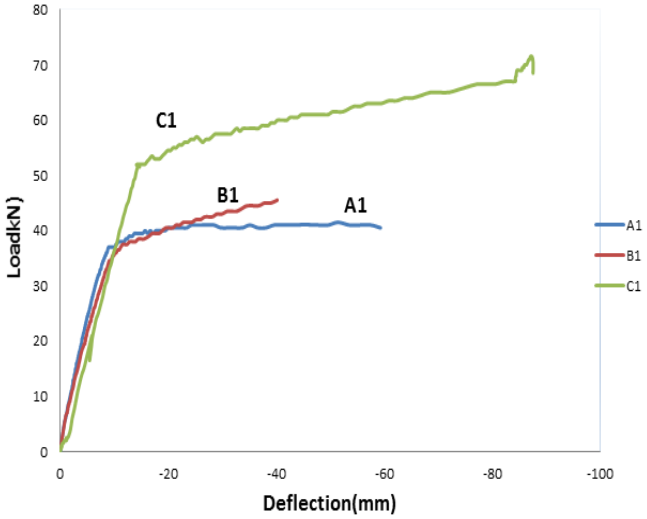

Figure 6 a: Load versus midspan deflection of the control beams A1, B1, and C1.

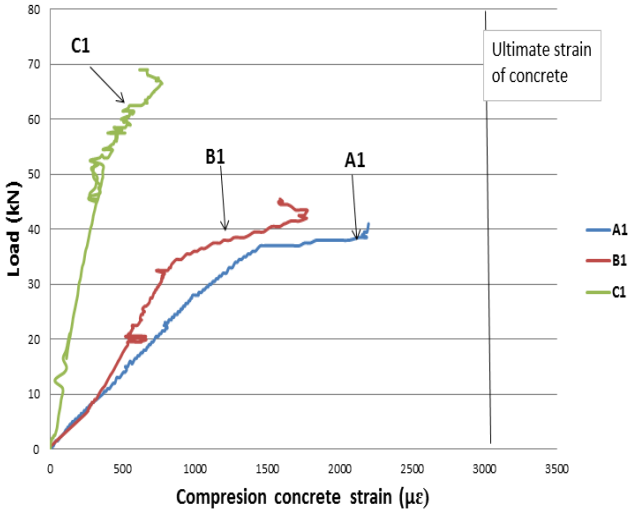

Figure 6 b: Load versus compression strain for the control beams A1, B1, and C1.

3.2.2. Strengthened beams

The results include the load versus midspan deflection curves; measured and 'average' strains; and a description of the failure mode.

A considerable increase of the measured maximum load was observed due to the addition of the CFRP and GFRP sheets for the strengthened beams A2, A3, B2 and C2 as shown in Fig. 7. The maximum load of the beams achieved was 55.5, 48.0, 56.5, 87.5 kN, respectively. The strengthening with CFRP and GFRP for the tested specimens A2, A3, B2 and C2 lead to increase the load capacity compared to the unstrengthened control beam by 35.4%, 17.1%, 25.3% and% 22.4%, respectively. However, strengthened beams failed due to debonding of the CFRP sheets from the beams.

3.2.2.1. Small scale strengthened beams

Mode of failure for strengthening beams "A2 and A3" is shown in Fig. 8. For beam type A2 a linear response up to the cracking load of 12.0 kN. Almost identical cracks occurred around the middle of the beam at the start of the shear crack at load 45 kN (80%) of the total load at a distance of 300 mm from the support, and a long inelastic response up to the ultimate load of 55.5 kN.

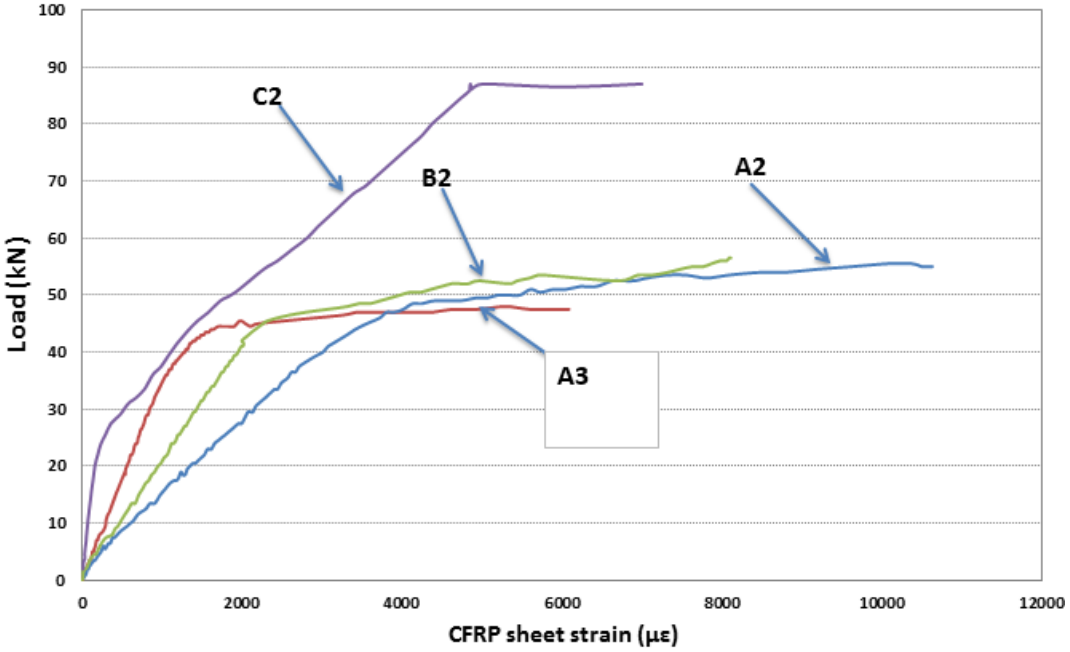

Figure 7: Load versus FRP strain for strengthened beams with end anchorage.

Figure 8 a: Mode of failure for beam A2.

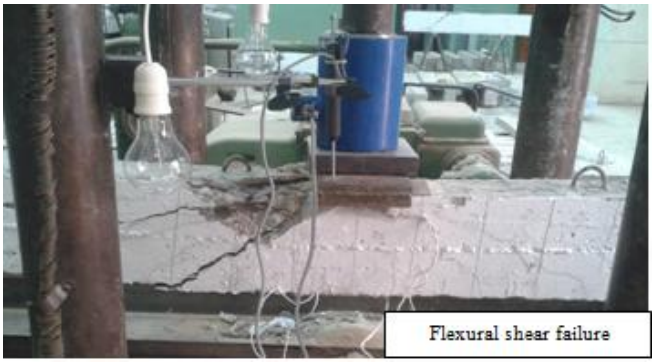

Figure 8b: Mode of failure for beam A3.

Loading of beam A2 was stopped at a deflection of about 29.9 mm (1/60 of the span) and mm. The strain in the CFRP strips measured immediately prior to debonding failure was 10631 με which corresponded to nearly 75% of their ultimate tensile strain of the CFRP. As referred in the literature review, the premature debonding resulted in hardly utilizing the full material capacity of FRP reinforcement.

For beam type A3 a linear response up to the cracking load of 11.0 kN. Almost identical cracks occurred around the middle of the beam up the start of the shear crack at load 33 kN (69%) of the total load at 300 mm from the support, and a long inelastic response up to the ultimate load of 48 kN. Loading of beam A3 was stopped at a deflection of about 28.67 mm (1/63 of the span). The strain in the GFRP strips was measured immediately prior to debonding failure was 7640 με which corresponded to nearly 27.28 % of their ultimate tensile strain of the GFRP, where the ultimate tensile strain equal 28000 με. Maximum strain value for A3 was very small as a result of the shear crack in the shear span and this led to the flexural shear failure. As referred in the literature review, the premature debonding resulted in hardly utilizing the full material capacity of FRP reinforcement. The cracking pattern of beam A2 and A3 includes vertical flexural cracks around midspan and diagonal shear–flexure cracks in the constant shear spans. Such diagonal cracks have not been observed in beam A1(unstrengthened beam) and are attributed to the reduced amount of shear reinforcement. Failure of beam A2 occurred due to debonding of CFRP sheet and the mode of failure for A3 was a flexural shear failure. As shown in Fig.8.

From Fig. 9. The strengthening using CFRP have the highest efficiency of the beam to resist all types of loads than using strengthened GFRP with an increase in efficiency by 35.60% and 17.07 % respectively.

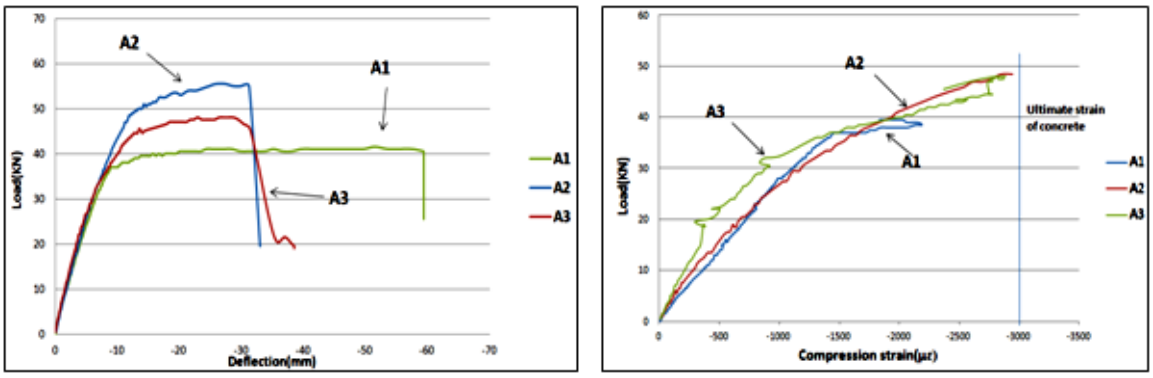

Figure 9a: Load versus midspan deflection & concrete compression strain for the beams A1, A2 and A3.

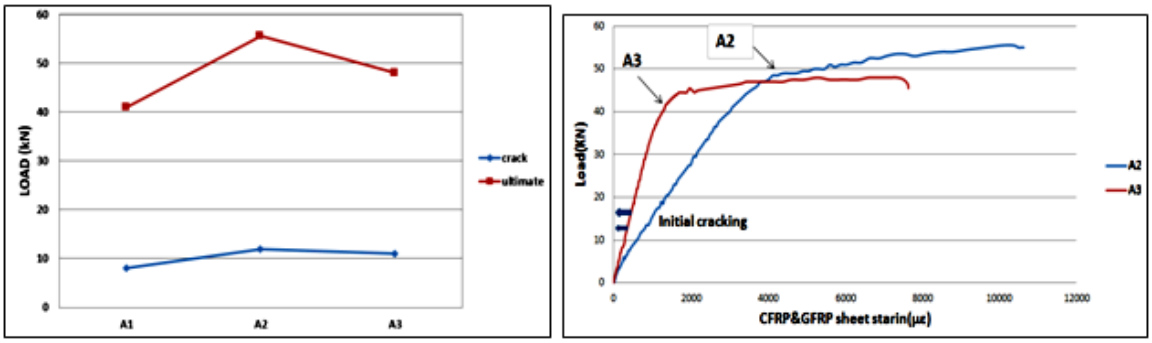

Figure 9b: Comparison between tested beams A2 and A3.

3.2.2.2. Size effect on the nominal strength of geometrically scaled beams

Three different sizes in length and cross section beams were tested (A2, B2, C2), while keeping the width of CFRP constant for a width of the section (bf=2/3 b) and reinforcement ratio of CFRP sheets was constant for area of tensile steel reinforcement (Af= 10 % As).

It is noticed that the strengthening of beams by using the fiber led to increase the moment capacity of sections and increase the value of the first cracking load in all cases.

The CFRP sheets increased the first-cracking load of beams A2, B2 and C2 by 50%, 20% and 10 %, respectively, and the ultimate load by 35.36%, 25.27% and 22.38% respectively. As it is clear, smaller size of the beam, the higher increase in the ultimate load, as shown in Fig. 10. a.

If one looks at the deflection ductility and energy ductility indices of the CFRP strengthened beams, it is obvious that as the beam size decreases the ductility of beams increases as shown in Fig10. b. The mode of failure of strengthening beams (B2 and C2) is shown in Fig. 10. c. and the mode of failure for beam A2 was shown in Fig. 8. a. A comparison was made between the experimental results for the ultimate strain in the CFRP for intermediate flexural crack-induced debonding. Fig. 10.d. showed the maximum strain of CFRP sheets at different size.

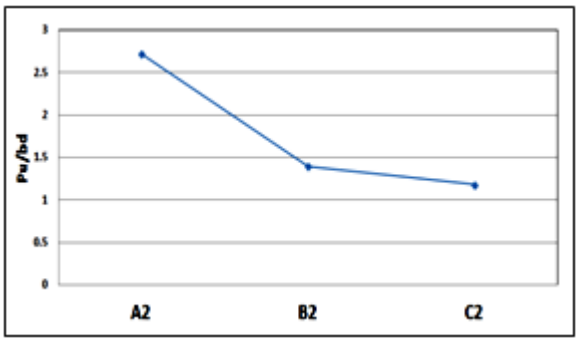

Figure 10 a: Stress at ultimate load as a function of beam size.

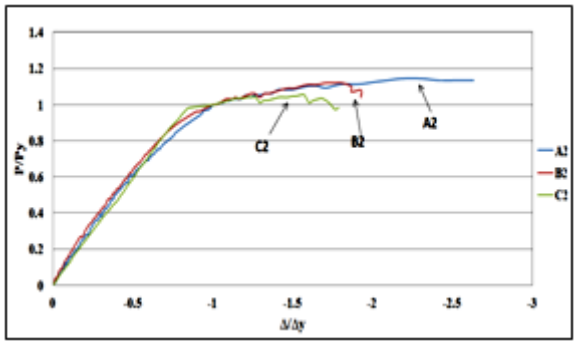

Figure 10 b: Normalized load-midspan displacement curve for beams "A2, B2 and C2".

Figure 10.c: Mode of failure for strengthening beams B2 and C2

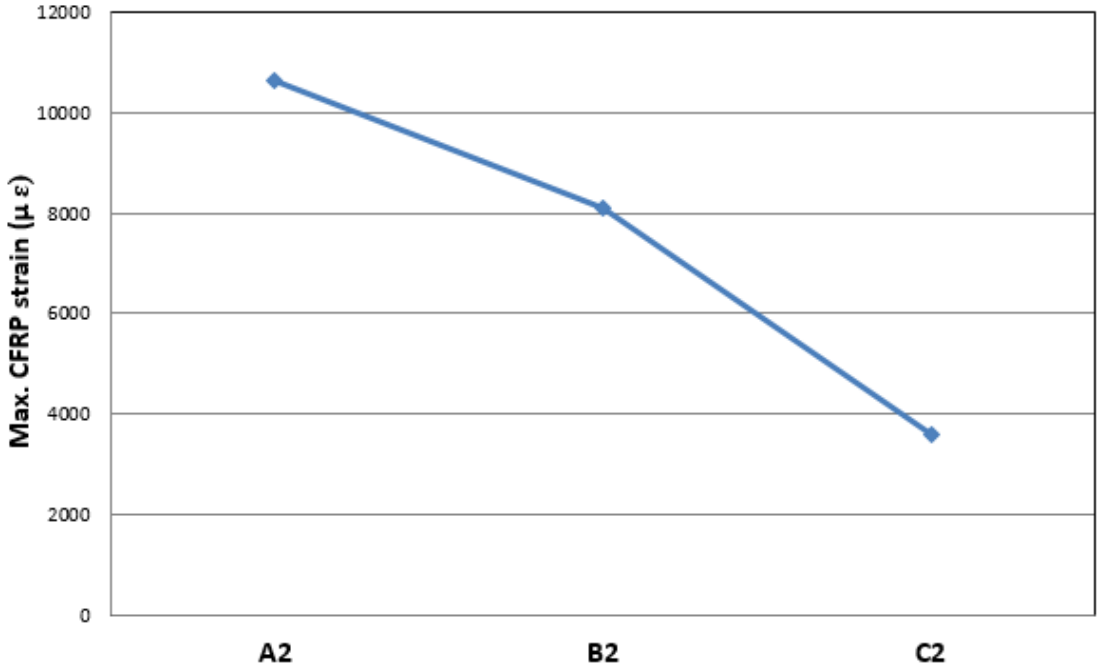

Figure 10.d: Max. CFRP strain for strengthened beams A2, B2 and C2

4. Analytical Results

According to [18], the following assumptions are made in calculating the nominal flexural strength of RC beams strengthened with CFRP&GFRP sheets:

- As the ultimate compressive strain in concrete reaches 0.003, concrete stress of (0.67 $f$cu) shall be assumed uniformly distributed over an equivalent compression zone bounded by edges of the cross section and a straight line located parallel to the neutral axis at a distance (a = β1 c) from the fiber of maximum compressive strain, where C is the actual depth of the compression zone, and the parameter β can be determined according to ACI 318-08 [19].
- Reinforcing steel is assumed to behave elastic-perfectly plastic response, and the FRP sheet has a linear elastic stress–strain relationship up to failure.
- The shear deformation within the adhesive layer is neglected since the adhesive layer is very thin with slight variations in its thickness**.**
- The tensile strength of concrete is ignored.

4.1. Tension failure and debonding failure

The balanced CFRP reinforcement ratio of strengthening section "ρfb" can be implied from Eq. (1), and FRP reinforcement ratio ρf = Af/bd.

Strengthened beams with a CFRP reinforcement ratio, ρf < ρfb, fail by the rupture or debonding of CFRP sheet prior to the concrete crushing in compression zone

$$\rho_{fb} = \frac{A_{fb}}{bd} = \frac{.67 * f_{cu*} \ b * a_{b-} A_{s*} f_y + A_{s`*} f_{y`}}{bd_* f_{fu}} \quad (1)$$

Where, a: the depth of the equivalent rectangular concrete stress block.
Referring to fig. 11, the strain conditions in the cross section satisfy εf= [εfu] and (εc < εcu). In this case, the concrete strain will not reach 0.003 at failure of the strengthened beam, and the use of the rectangular stress block assumption would not be valid. Based on the assumption of linear strain distribution, the following equations can be obtained:

$$a = \frac{A_{f*} f_{fu} + A_{s*} f_y}{.67 * f_{cu*} \ b} \quad (2)$$

$$Mn_{=}A_{s*}\,f_y(d-\frac{a}{2})+A_{f*}\,f_f(t-\frac{a}{2}) \quad (3)$$

Where $f_f = k_m\varepsilon_{fu}\ {}^{*}E_f$. (4)

In Eq. (4), the item of $k_m\varepsilon_{fu}$ represents the strain increase limitation for the FRP sheet, which can be determined by Eq. (5) proposed for preventing the debonding failure of nonprestressed FRP sheet in ACI 440.2R-02 [20].

$$k_m\varepsilon_{fu} = \begin{cases} \frac{1}{60}\left(1-\frac{nE_f t_f}{360.000}\right) \le 0.90\,\varepsilon_{fu} & \text{for } nE_f t_f \le 180.000 \\ \frac{1}{60}\left(\frac{90.000}{nE_f t_f}\right) \le 0.90\,\varepsilon_{fu} & \text{for } nE_f t_f > 180.000 \end{cases} \quad (5)$$

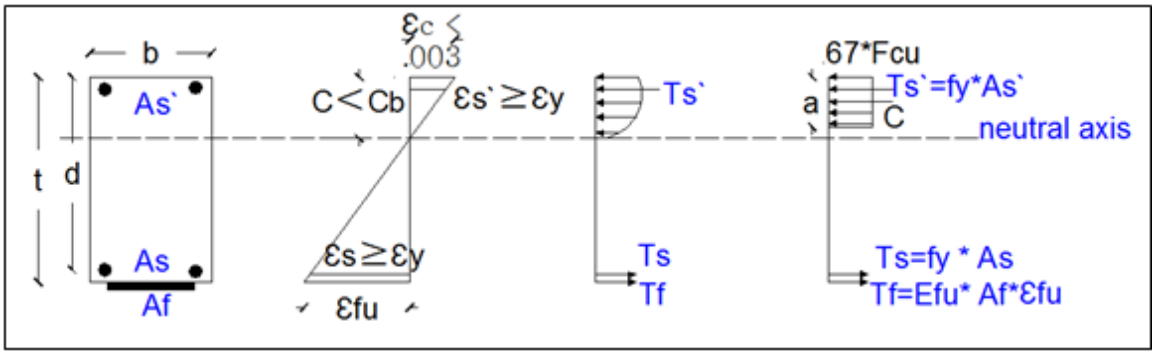

Figure 11. Internal strain and stress distribution for the strengthened section under the debonding failure or tension failure

4.2. Verifications

The experimental and calculated results are shown in Table 5 and Fig.12 for all the tested specimens:

Table 5: Comparison between the experimental and calculated results

Specimen	Mcr (kN.M)			Mn (kN.M)		
	Cal.	Exp.	Exp./Cal.	Cal.	Exp.	Exp./Cal.
A2	2.94	5.40	1.84	23.25	24.98	1.07
A3	2.94	4.95	1.68	17.27	21.60	1.25
B2	8.28	8.40	1.01	39.48	39.55	1.00
C2	19.63	21.5	1.10	92.41	94.06	1.02

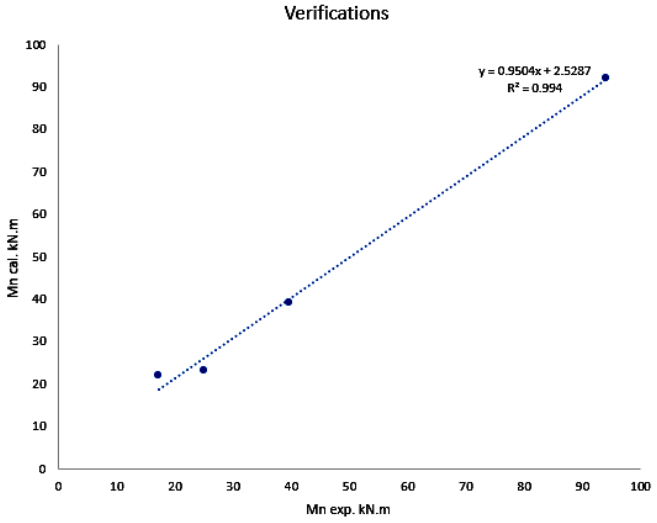

Figure 12: Comparison between the experimental and calculated results

5. Conclusions

In this study, experimental work for development of the flexural capacity of R C beams strengthened with the CFRP and GFRP sheets has been carried out. The analytical evaluation is verified with the experimental results, and the feasibility of the model is certified. The conclusions of this paper are summarized as follows:

1. It is confirmed that, compared with control specimen, surface bonding with a CFRP sheet increases the ultimate load of the tested specimens up to 35 %and for GFRP increases the ultimate load of a specimen as much as 17%,.
2. IC" Intermediate Crack" debonding failure occurred at about 70% of the ultimate strain of CFRP and no anchorage deboning notice of all beams the beam as a result of using the anchorage.
3. CFRP can effectively increase initial cracking loads, ultimate loads and stiffness of the tested concrete beams and, also, improves crack patterns compared with unstrengthened beams. The CFRP sheets increased the first-cracking load of beams A2, B2 and C2 by 50%, 20% and 10 %, respectively, and the ultimate load by 35.36%, 25.27% and 22.38% respectively
4. Debonding failure of concrete beams strengthened with CFRP and GFRP occurs before the ultimate load which corresponds to FRP rupture, so, the high strength property of CFRP and GFRP cannot be fully utilized.
5. Efficiency of FRP-strengthened beams depending on the axial stiffness of FRP, where the stiffness of CFRP sheet is higher than the stiffness of GFRP sheet, so, it is confirmed that, using the CFRP sheets in the strengthening gives double efficiency compared to using GFRP in spite of the economic cost of the last.
6. The beam size has significantly influenced the strengthening ratio, where the small size gives higher efficiency with strengthening method, and the beam size decreases as the ductility increases.
7. A comparison between the measured results and analytical results based on the equilibrium of forces and compatibility of strains indicated that the behavior of upgrading beams can be predicted with reasonable accuracy. However, additional analytical and experimental studies must be undertaken to establish criteria for predicting the limiting load that causes the

failure of the concrete layer between the longitudinal rebars and sheet.

Appendix A. Notation

The following symbols are used in this paper:

A_f	Area of CFRP plates corresponding to the balanced ratio.
A_s	Area of tensile steel reinforcement.
$A_s`$	Area of compressive steel reinforcement.
A	Depth of the equivalent rectangular compression block.
B	Width of the rectangular beam section.
C	Depth of the neutral axis.
C_b	Depth of neutral axis in section with a balanced ratio.
D	distance from centroid of outermost tensile steel reinforcement to extreme concrete compression fiber
E_c	modulus of elasticity of concrete
E_s	modulus of elasticity of tensile steel reinforcement
E_f	tensile modulus of elasticity of FRP sheet
f_{fu}	ultimate tensile strength of FRP sheet
f_y	yield strength of tensile steel reinforcement
$f_{y`}$	yield strength of compressive steel reinforcement
K_m	reduction factor
M_n	nominal flexural strength of the strengthened beam without taking into account the reduction factor
β1	factor relating depth of equivalent rectangular compressive stress block to neutral axis depth
ε_c	compressive strain in concrete
ε_{cu}	ultimate compression strain in concrete (0.003)
ε_{fu}	nominal ultimate tensile strain of the FRP sheet
ρ_f	FRP reinforcement ratio
ρ_{fb}	balanced FRP reinforcement ratio

References

[1] Elnashai, A. (2002): "Evaluation of Strengthened RC Buildings" Proceedings of seminar on the use of FRP in civil engineering، Cairo- Egypt. PP. 260–266.

[2] Rizkala, S. and Labossiere. (1999)."Structural Engineering with FRP in Canada" Concrete International Magazine، PP. 27-30.

[3] Salama, A. and Abdel Naby, S. (2000):"The Use of FRP in Structural Elements" International workshop on structural composites for infrastructures application، Cairo-Egypt، PP. 165-180.

[4] Diab, H. M. and. Farghal, O. A (2014): "Bond strength and effective bond length of FRP sheets/plates bonded to concrete considering the type of adhesive layer." Elsevier Composites: Part B 58: 618-624.

[5] Abdelhady, H.; Amr, H. S. and Elafandy, T. (2006): "Performance of reinforced concrete beams strengthened by hybrid FRP laminates." Cement and Concrete Composites 28: 906- 913.

[6] April, A. and Spacone, E. (2001): "Role of bond in RC beams strengthened with steel and FRP plates." J. Struct. Eng. 127: 1445- 1452.

[7] Guo, Y.C.; Liu, F. and Bungey, J. H. (2006): "An experimental and numerical study of the effect of thickness and length of CFRP on performance of repaired reinforced concrete beams." Construction and Building Materials 20:901-909.

[8] Saadatmanesh, H. A. (1992): "RC beams strengthened with GFRP plates. I: Experimental study". Journal of Structural Engineering. 117: 34 17:3433.

[9] Attari, N. and Amziane, S. (2012): "Flexural strengthening of concrete beams using CFRP, GFRP and hybrid FRP sheets." Construction and Building Materials 37: 746-757.

[10] Fanning, P. J. and Kelly, O. (2001): "Ultimate response of RC beams strengthened with CFRP plate." J. Compos. Constr 5: 122_127.

[11] Shahawy, M. and Beitelman, T. E. (1999):"Static and fatigue performance of RC beams strengthened with CFRP laminates." J. Struct. Eng. 125: 613_621.

[12] Rahimi, H. and Hutchinson, A. (2001): "Concrete beams strengthened with externally bonded FRP plates" J. Compos. Constr. 5: 44-56.

[13] Smith, S. T. and Teng, J. G. (2002):"FRP-strengthened RC beams. II: assessment of debonding strength models." Engineering Structures 24: 397–417.

[14] Galal, K. and Mofidi, A. (2010): "Shear strengthening of RC T-beams using mechanically anchored unbonded dry carbon fiber sheets." J. Perform. Constr. Facil., 24, 1: 31–39.

[15] Al-Mahaidi, R. and Sentry, M. W. G. (2009):"Testing the efficiency of anchorage systems applied to CFRP laminate strips bonded to concrete-Westgate bridge strengthening project." Dept. of Civil Engineering Rep., Monash Univ., Melbourne, Australia.

[16] Kim, S. J. and Smith, S. T. (2010): "Pullout strength models for FRP anchors in uncracked concrete." J. Compos. Constr., 14, 4: 406–414.

[17] Maalej, M. and Leong, K. S. (2005): "Effect of beam size and FRP thickness on interfacial shear stress concentration and failure mode of FRP Strengthened beams" Composites Science and Technology 65: 1148-1158.

[18] Xue, W., Y. Tan. (2010). "Flexural response predictions of reinforced concrete beams strengthened with prestressed CFRP plates" Composite Structures 92: 612-622.

[19] ACI Committee 318. (2008): "Building code requirements for structural concrete (ACI 318-05) and commentary (ACI 318-05)." Rep., American Concrete Institute (ACI), Farmington Hills, MI.

[20] ACI Committee 440. Guide for the design and construction of externally bonded FRP systems for strengthening concrete structures (ACI 440.2R-02). Farmington Hills, MI: American Concrete Institute; 2002. p. 45.